Electronic Supporting Information

Promoting Photoluminescence Quantum Yields of Glass-Stabilized $CsPbX_3$ (X=Cl, Br, I) Perovskite Quantum Dots through Fluorine Doping

Daqin Chen [a,c,d,*], Yue Liu[b], Changbin Yang[a,c,d], Jiasong Zhong [b,*], Su Zhou[b], Jiangkun Chen[a,c,d], Hai Huang[a,c,d]

[a]College of Physics and Energy, Fujian Normal University, Fujian Provincial Key Laboratory of Quantum Manipulation and New Energy Materials, Fuzhou, China
E-mail: dqchen@fjnu.edu.cn

[b]College of Materials & Environmental Engineering, Hangzhou Dianzi University, Hangzhou, 310018, China
E-Mai: jiasongzhong@hdu.edu.cn

[c]Fujian Provincial Collaborative Innovation Center for Optoelectronic Semiconductors and Efficient Devices, Xiamen, 361005, China

[d]Fujian Provincial Engineering Technology Research Center of Solar Energy Conversion and Energy Storage, Fuzhou, China

Experimental Section

Synthesis of $CsPbX_3$ PQDs@glass. The present nanocomposites were prepared by a traditional melt-quenching and subsequent heat-treatment. Oxyhalide borosilicate glasses were designed with the compositions of SiO_2-B_2O_3-ZnO-Cs_2CO_3-PbX_2-NaX (X=Cl, Br, I and their mixtures) and fluorine doping was realized by introducing NH_4F, LiF, NaF, CaF_2, PbF_2, YF_3 or LuF_3 into glass. The raw materials were mixed well and ground into powders for a certain of time, and melted in a muffle furnace at 1150~1200℃ for 8~50 min under ambient atmosphere to prepare precursor glass. Finally, $CsPbX_3$ PQDs@glass was obtained through in-situ glass crystallization via heat-treatment at 460~580 ^{o}C for 2 h.

Structural Characterizations. XRD analysis was carried out to identify the phase structure of the as-prepared samples using a powder diffractometer (MiniFlex600 RIGAKU) with Cu K_{α} radiation (λ= 0.154 nm) operating at 40 kV. FTIR spectra were measured via a Perkin-Elmer IR spectrometer using the KBr pellet technique. Raman spectra were determined by a LabRam HR Raman spectrometer operated with 633 nm as excitation source. ^{28}Si, ^{11}B and ^{19}F magic angle spinning (MAS) nuclear magnetic resonance (NMR) spectra were performed using a Bruker ADVANCE III HD 400 instruments. Microstructure observations of $CsPbX_3$ PQDs@glass were carried out on a JEOL JEM-2010 TEM operated at 200 kV accelerating voltage. STEM images were taken on a FEI aberration-corrected Titan Cubed S-Twin transmission electron microscope operated on a HAADF mode.

Spectroscopic Characterizations. Photoluminescence (PL) spectra were recorded on an Edinburgh Instruments (EI) FLS1000 spectrofluoremeter equipped with continuous (450 W) xenon lamps. Time-resolved PL traces for exciton emission of $CsPbX_3$ PQDs were detected on a fluorescent lifetime spectrometer (Edinburgh Instruments, LifeSpec-II) based on a time correlated single photon counting technique under the excitation of 375 nm picosecond laser. The optoelectronic parameters for the PQD phosphors-converted LEDs, including LE, CRI, CCT and Commission Internationale de L'Eclairage (CIE) color coordinates, were measured by using a sphere-spectroradiometer system consisting of an integrating sphere (30 cm in diameter, Labsphere Inc., USA) and a CCD spectrometer (CDS2100, Labsphere Inc., USA).

Absolute photoluminescence Quantum yield (PLQY), defined as the ratio of emitted photons to absorbed ones, was measured by a spectrofluoremeter (FS1000). An integrating sphere was mounted on the spectrofluoremeter with the entrance and exit ports located in 90^{o} geometry. The PQD sample was located in the center of the integrating sphere. All the recorded spectroscopic data were corrected for the spectral responses of both the spectrofluoremeter and the integrating sphere. The responses of the detecting systems (integrating sphere, monochromators and detectors) in photon flux were determined using a calibrated tungsten lamp. Based on this setup, PLQY is calculated based on the following equitation

$$\eta = \frac{\text{number of photons emitted}}{\text{number of photons absorbed}} = \frac{L_{sample}}{E_{reference} - E_{sample}} \quad (1)$$

where η represents QY, L_{sample} the emission intensity, $E_{reference}$ and E_{sample} the intensities of the excitation light not absorbed by the reference and the sample respectively. The difference in integrated areas between the sample and the reference represents the number of the absorbed photons. The emitted photons were determined by integrating the related emission band.

Table S1 Summary of PLQY values for the $CsPbX_3$ (X=Cl, Br, I) PQDs@glass samples prepared by different research groups.

PQDs@glass	PL peak wavelength	PLQY	reference
$CsPbCl_3$	410 nm	Un-detectable	[1]
$CsPbCl_3$	407 nm	3%	This work
$CsPbBr_3$	521 nm	51.5%	[2]
Eu^{3+}:$CsPbBr_3$	520 nm	73.5%	[3]
$CsPbBr_3$	522 nm	70%	[4]
$CsPbBr_3$	530 nm	81.1%	[5]
$CsPbBr_3$	520 nm	80%	This work
$CsPbBrI_2$	640 nm	20.2%	[5]
$CsPb(Br/I)_3$	580~650 nm	50~60%	This work
$CsPbI_3$	690 nm	4.2%	[6]
$CsPbI_3$	688 nm	50%	This work

[1] D. Chen, S. Yuan, J. Chen, J. Zhong, X. Xu, Robust $CsPbX_3$ (X=Cl, Br, and I) perovskite quantum dot embedded glasses: nanocrystallization, improved stability and visible full-spectral tunable emissions. *J. Mater. Chem. C* **2018**, *6*, 12864-12870.

[2] B. Ai, C. Liu, J. Wang, J. Xie, J. J. Han, X. J. Zhao, Precipitation and optical properties of $CsPbBr_3$ quantum dots in phosphoate glasses. *J. Am. Ceram. Soc.* **2016**, *99*, 2875-2877.

[3] R. Yuan, L. Shen, C. Shen, J. Liu, L. Zhou, W. D. Xiang, X. J. Liang, $CsPbBr_3$:xEu^{3+} perovskite QD borosilicate glass: a new member of the luminescent material family. *Chem. Commun.* **2018**, *54*, 3395-3398.

[4] S. Yuan, D. Chen, X. Li, J. Zhong, X. Xu, In Situ crystallization synthesis of $CsPbBr_3$ perovskite quantum dots embedded glasses with improved stability for solid-state-lighting and random upconverted lasing. *ACS Appl. Mater. Interfaces* **2018**, *10*, 18918-18926.

[5] Y. Ye, W. Zhang, Z. Zhao, J. Wang, C. Liu, Z. Deng, X. Zhao, J. Han, Highly luminescence cesium lead halide perovskite nanocrystals stabilized in glasses for light-emitting applications. *Adv. Opt. Mater.* **2019**, *7*, 1801663.

[6] S. Liu, Y. Luo, M. He, X. Liang, W. Xiang, Novel $CsPbI_3$ QDs glass with chemical stability and optical properties. *J. Euro. Ceram. Soc.* **2018**, *38*, 1998-2004.

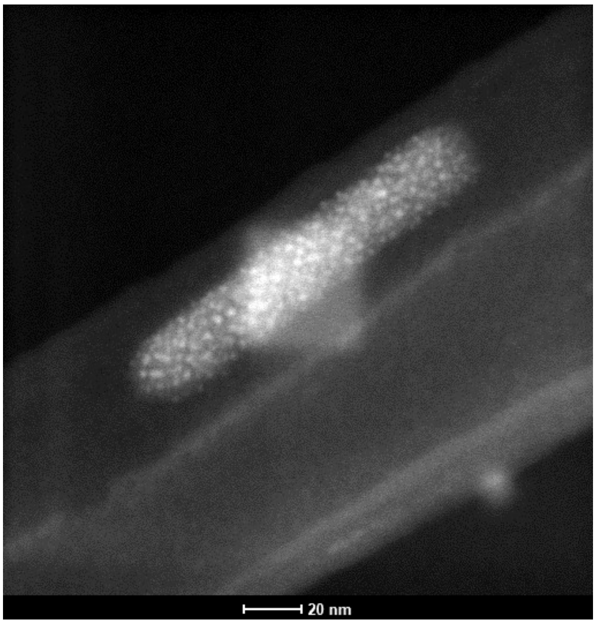

Figure S1 HAADF-STEM image of $CsPbCl_3$ PQDs@glass, showing homogenous distribution of $CsPbCl_3$ PQDs (bright) inside glass matrix (dark).

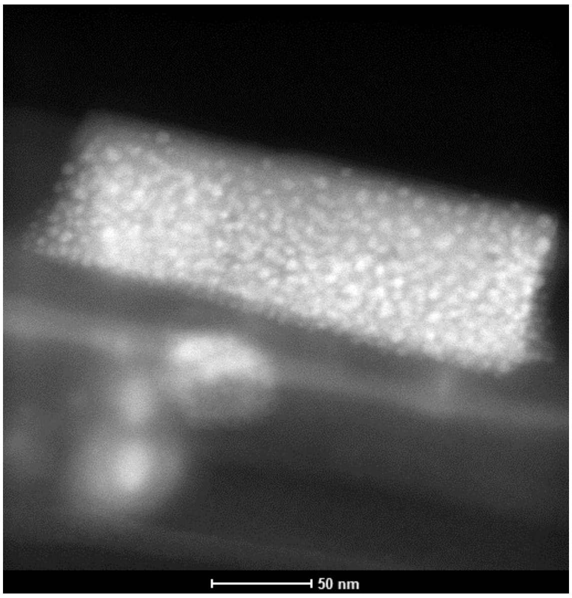

Figure S2 HAADF-STEM image of $CsPbBr_3$ PQDs@glass, showing homogenous distribution of $CsPbBr_3$ PQDs (bright) inside glass matrix (dark).

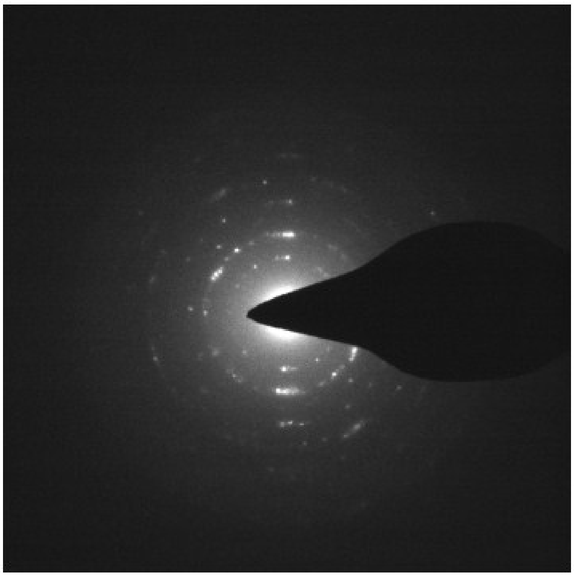

Figure S3 SAED pattern of $CsPbI_3$ PQDs@glass, showing diffraction rings of cubic $CsPbI_3$.

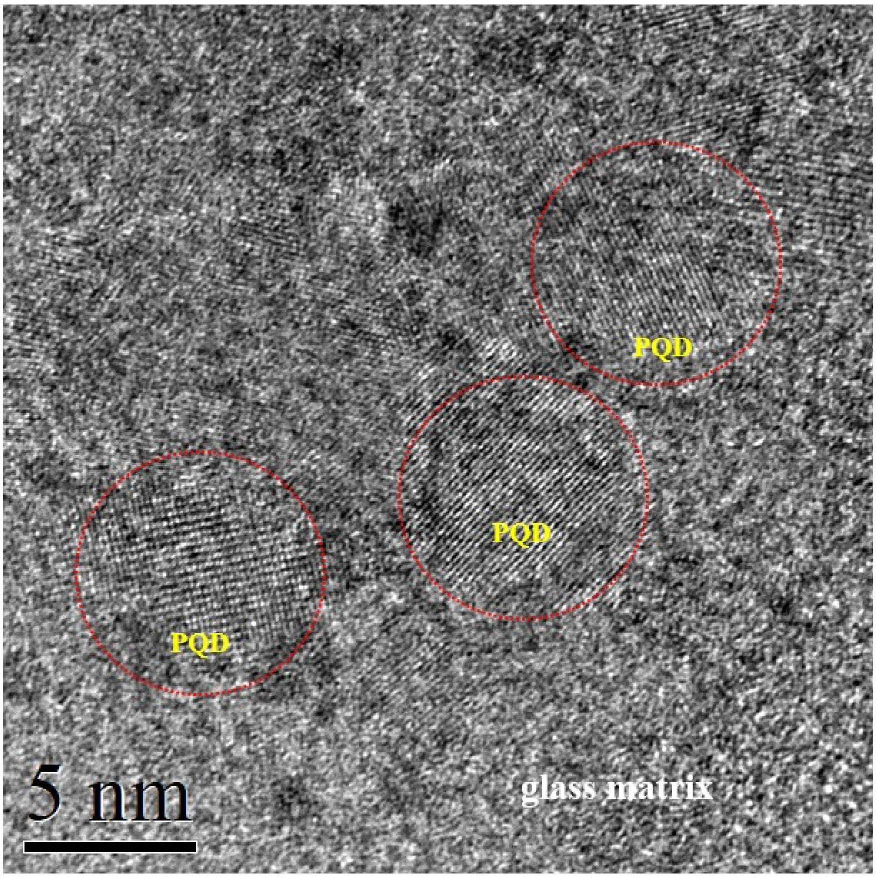

Figure S4 HRTEM micrograph of $CsPbI_3$ PQDs@glass, showing high crystallinity and distinctly resolved lattice fringes of cubic $CsPbI_3$ (red circles).

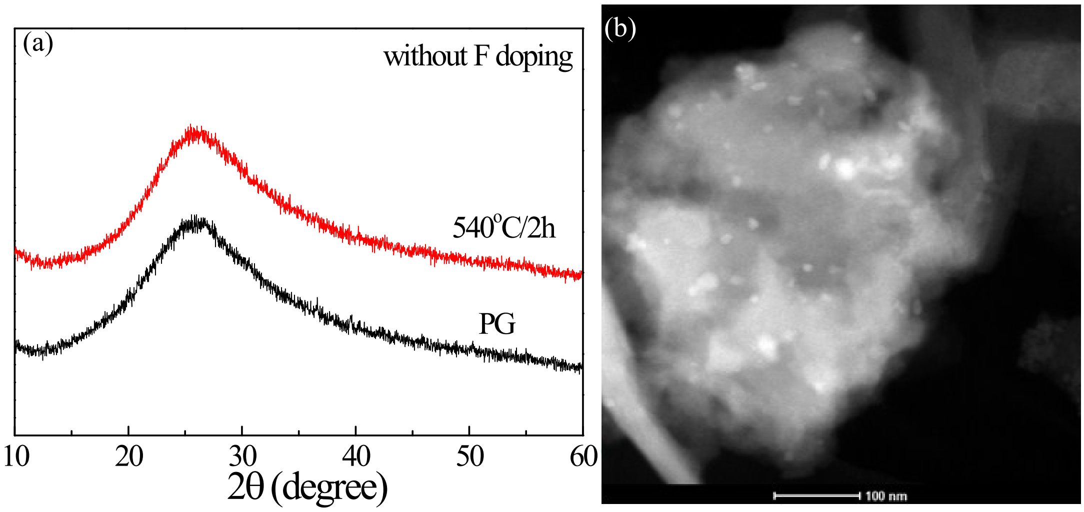

Figure S5 (a) XRD patterns of PG without F doping and the corresponding sample after heat-treatment at 580 ^{o}C for 2h. (b) HAADF-STEM image of the crystallized sample without F doping, showing that the amount of precipitated $CsPbI_3$ PQDs is little.

No obvious diffraction peaks of perovskite quantum dots are detected in XRD pattern of the heat-treated sample without F doping.

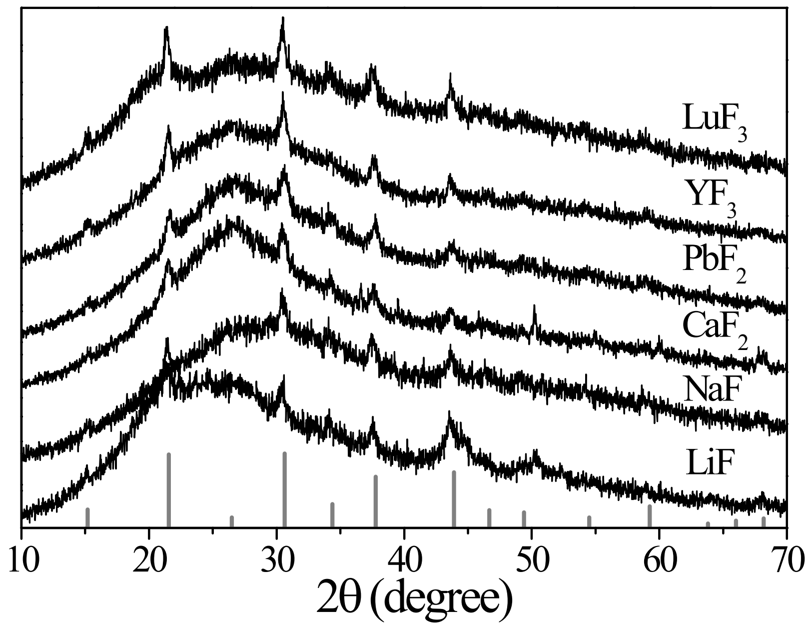

Figure S6 XRD patterns of $CsPbBr_3$ PQDs@glass samples with addition of various fluorides in PGs, evidencing the promoting role of fluoride additives for PQD precipitation from glass.

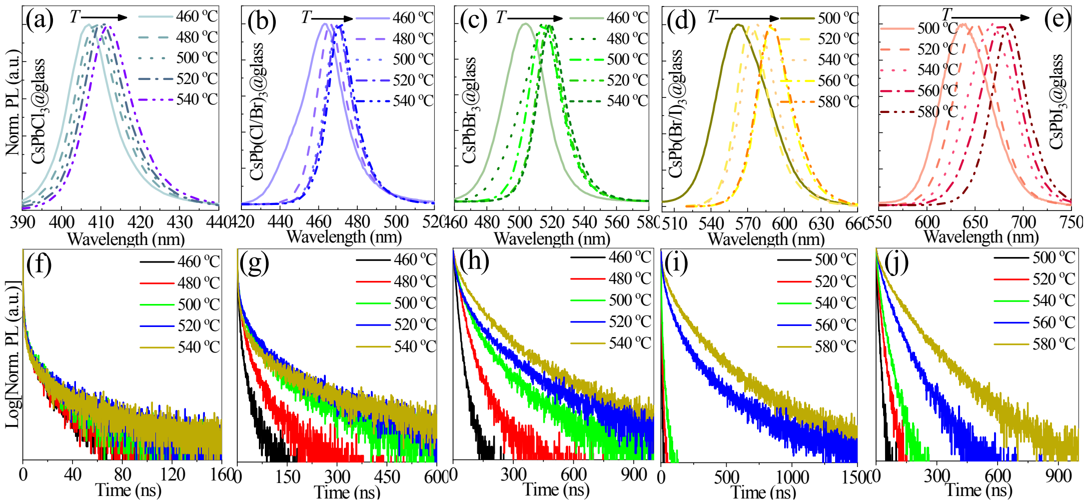

Figure S7 Crystallization temperature dependent PL spectra and time-resolved PL decays for $CsPbX_3$ PQDs@glass products: (a, f) X=Cl, (b, g) X=Cl/Br (Cl: Br=2.5: 0.5), (c, h) X=Br, (d, i) X=Br/I (Br: I=2: 1) and (e, j) X=I.

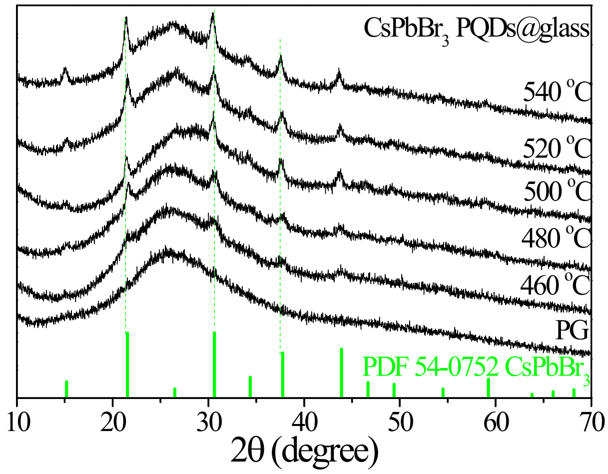

Figure S8 XRD patterns of PG and $CsPbBr_3$ PQDs@glass products prepared by heat-treatment at various temperatures for 2 h.

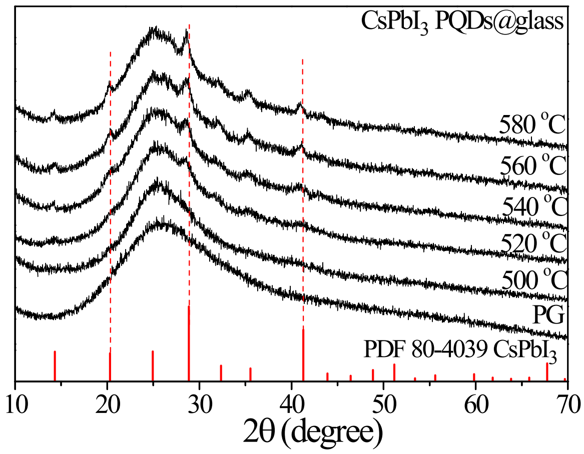

Figure S9 XRD patterns of PG and $CsPbI_3$ PQDs@glass products prepared by heat-treatment at various temperatures for 2 h.

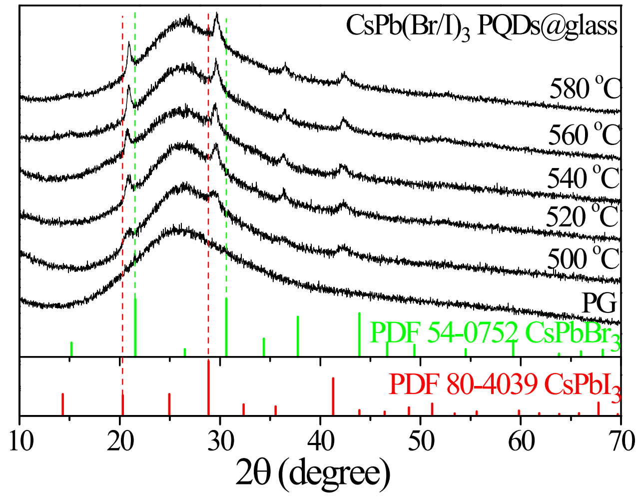

Figure S10 XRD patterns of PG and CsPb(Br/I)$_3$ PQDs@glass products prepared by heat-treatment at various temperatures for 2 h.

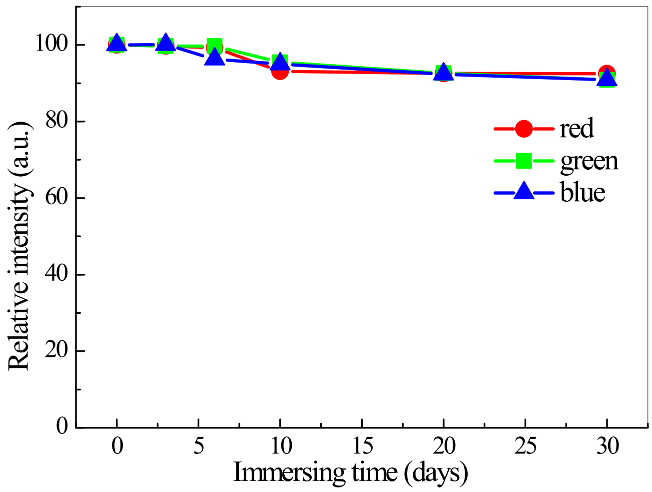

Figure S11 Relative PL intensities for blue $CsPbCl_{2.5}Br_{0.5}$, green $CsPbBr_3$ and red $CsPbBr_{1.5}I_{1.5}$ PQDs@glass samples versus immersing time in water.

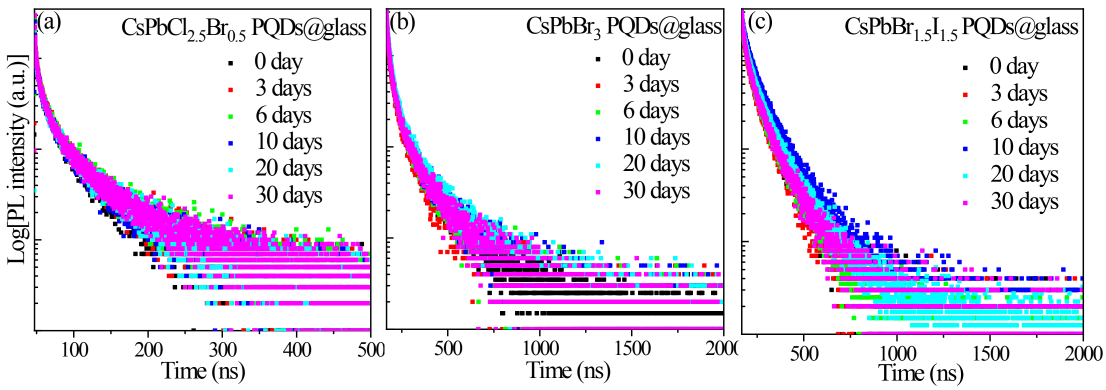

Figure S12 Time-resolved PL decays of the blue $CsPbCl_{2.5}Br_{0.5}$, green $CsPbBr_3$ and red $CsPbBr_{1.5}I_{1.5}$ PQDs@glass samples after immersing in water for different durations.

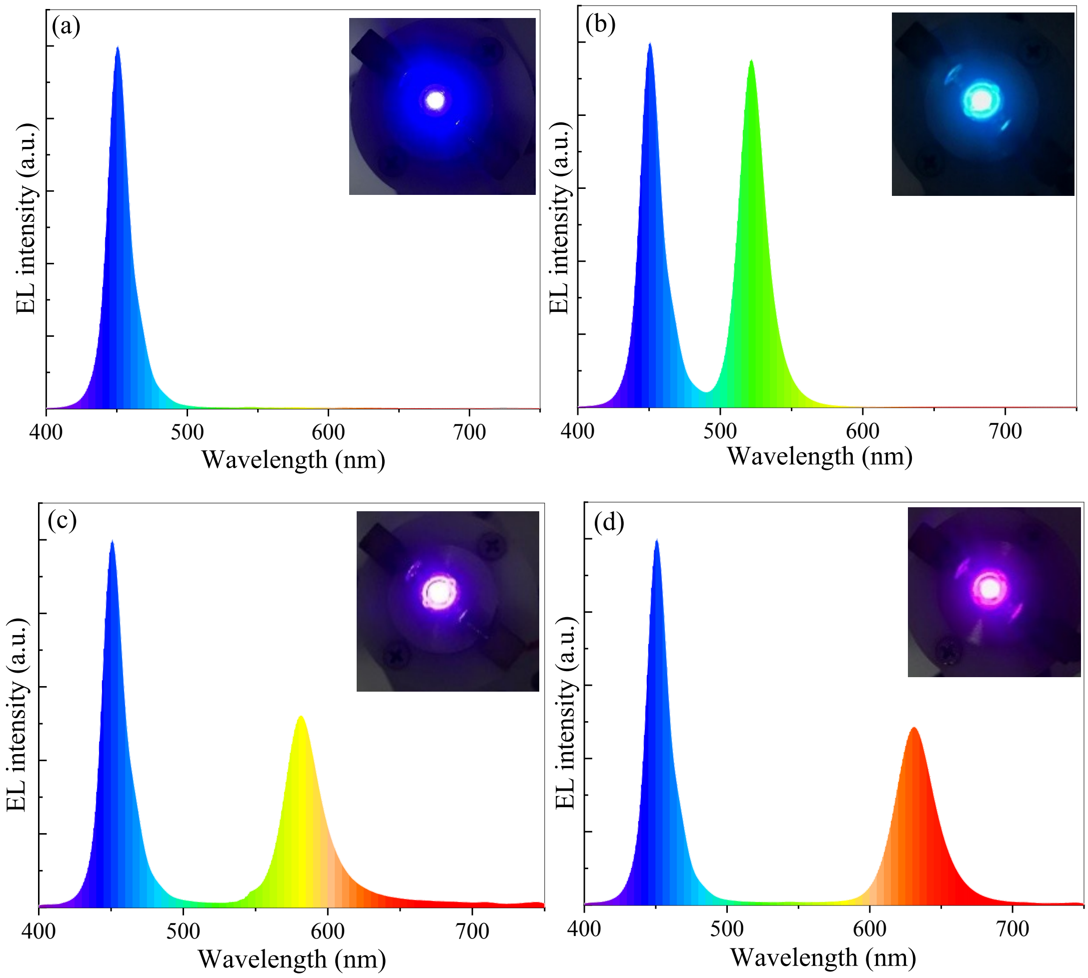

Figure S13 EL spectra of (a) InGaN blue chip and (b-d) LED devices fabricated by coupling blue chip with green $CsPbBr_3$ (520 nm), orange $CsPbBr_2I$ (580 nm) and red $CsPbBr_{1.5}I_{1.5}$ (630 nm) PQDs@glass phosphors, respectively. Insets are the corresponding LEDs driven by 100 mA operation current.

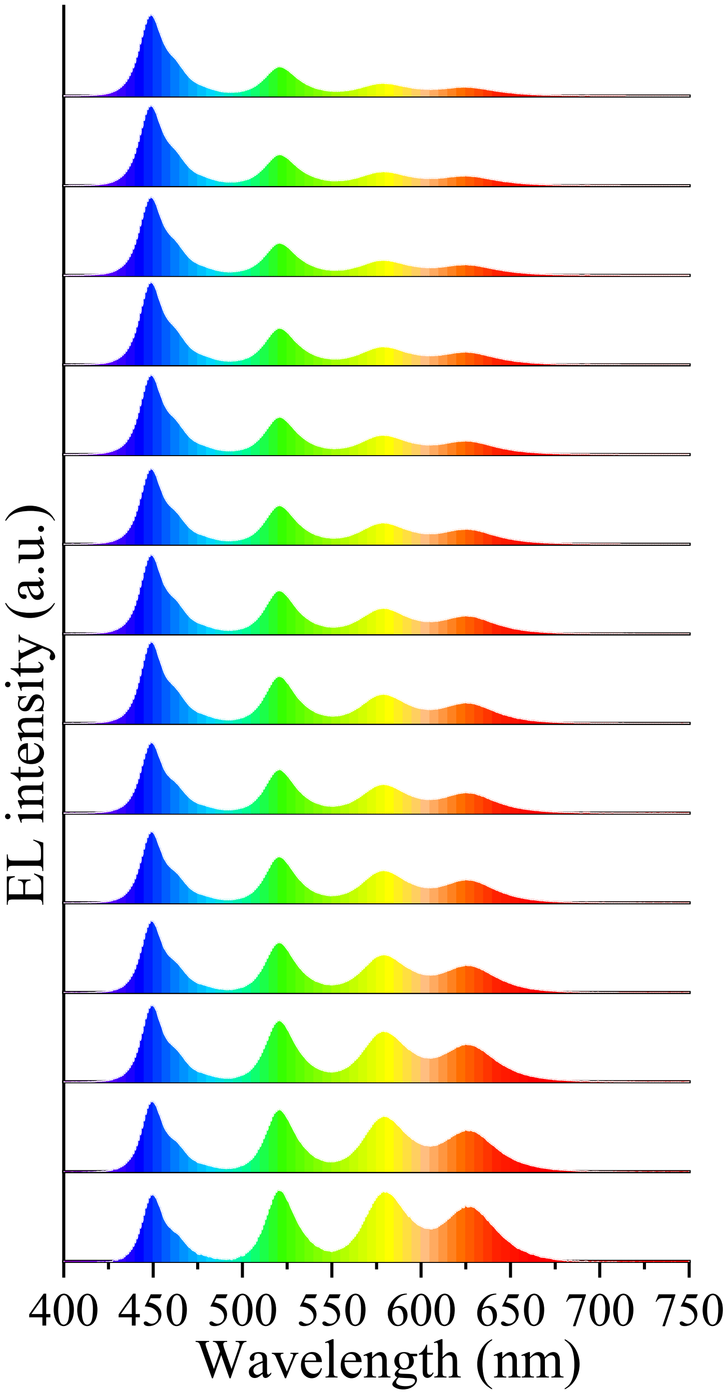

Figure S14 EL spectra of lighting devices constructed by coupling blue chip with green/orange/red ($CsPbBr_3$/$CsPbBr_2I$/$CsPbBr_{1.5}I_{1.5}$) PQDs@glass phosphors (from top to bottom: the amount of mixed green/orange/red PQD phosphors in device gradually increases). All the LEDs are driven by 100 mA operation current.

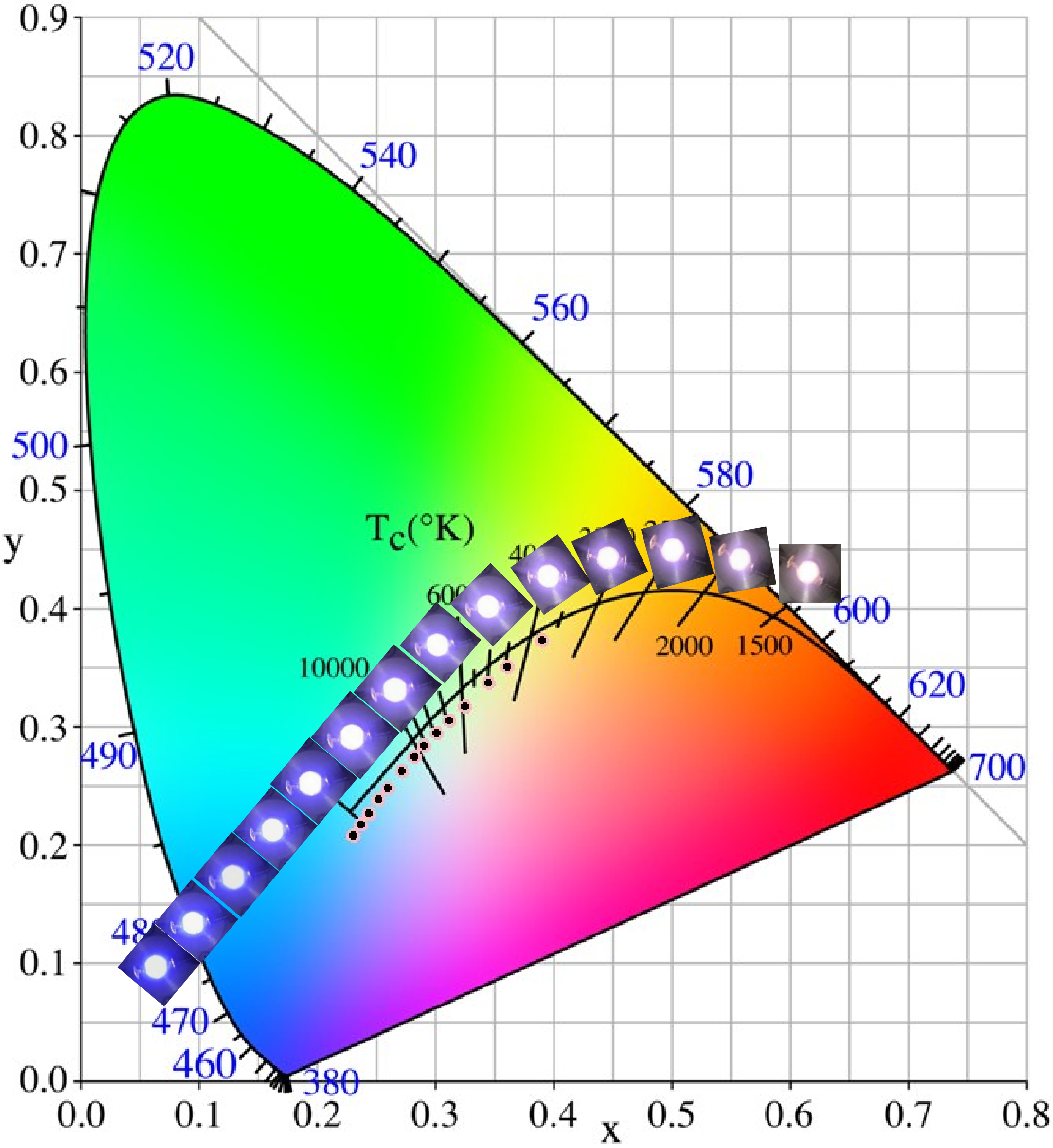

Figure S15 CIE Color coordinates of lighting devices constructed by coupling blue chip with green/orange/red ($CsPbBr_3$/$CsPbBr_2I$/$CsPbBr_{1.5}I_{1.5}$) PQDs@glass phosphors (from left to right: the amount of mixed green/orange/red PQD phosphors in device gradually increases). Insets are the corresponding devices driven under 100 mA operation current.

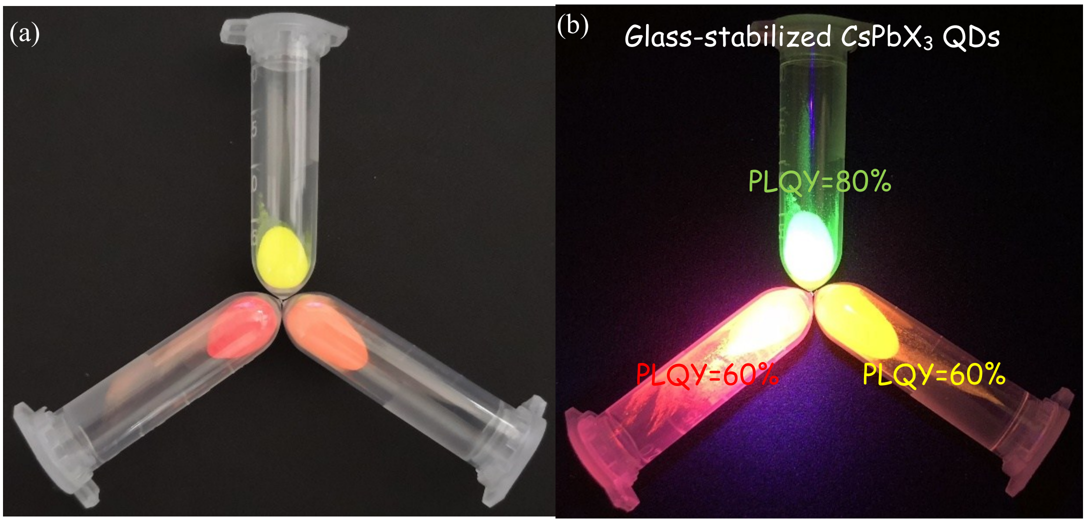

Figure S16 Photographs of glass-stabilized green, orange and red PQD phosphors with high PLQYs under (a) daylight and (b) the irradiation of UV light.

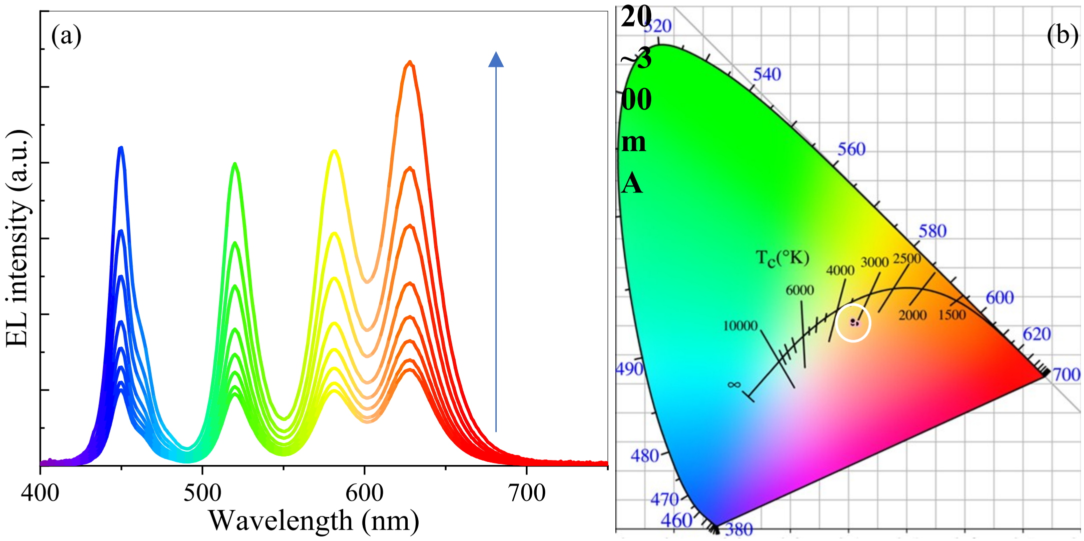

Figure S17 (a) Driven-current-dependent EL spectra and (b) the corresponding CIE color cooridates of white light-emitting diode fabricated by coupling blue chip with appropriate amount of green/orange/red ($CsPbBr_3$/$CsPbBr_2I$/$CsPbBr_{1.5}I_{1.5}$) PQDs@glass phosphors.